Research Square

Preprints are preliminary reports that have not undergone peer review.
They should not be considered conclusive, used to inform clinical practice,
or referenced by the media as validated information.

Contrasting Altitude and Long-term Geographical Isolation Shaped Phylogeography of Himalrandia lichiangensis, an Endemic Species from the Dry Hot Valley of Southwest China

Yaomei Qiao
Kunming Institute of Botany Chinese Academy of Sciences
Jian Liu
Kunming Institute of Botany Chinese Academy of Sciences
Xun Gong (gongxun@mail.kib.ac.cn)
Kunming Institute of Botany Chinese Academy of Sciences https://orcid.org/0000-0003-1705-6935

Research article

Keywords: Himalrandia lichiangensis, phylogeography, altitude, genetic differentiation, Sino-Himalayan Floristic Region, dry-hot valley

Posted Date: December 16th, 2020

DOI: https://doi.org/10.21203/rs.3.rs-126634/v1

License: This work is licensed under a Creative Commons Attribution 4.0 International License.
Read Full License

Abstract

Background: The eastern Sino-Himalayan region of southwest China, as one of the world's biodiversity hotspots, has undergone dramatic geomorphological and climatic changes during the Late Tertiary/Quaternary. The dry-hot valleys in southwest China is overlapping with the Hengduan Mountains. However, when this endemism was assembled in dry-hot valleys and how the climatic oscillations and/or tectonic movements influence their phylogeographical patterns remained largely unknown. *Himalrandia lichiangensis* is a shrub of Rubiaceae, endemically distributes in dry-hot valleys of southwest China. By integrating evidences from phylogeography, population dynamic and ecological niche modelling, we are aiming to trace the evolutionary history and explain the origin of biodiversity and endemism in the dry-hot valleys of southwest China.

Results: Based on sequencing four chloroplastic non-coding regions (*psb*M-*trn*D, *trn*D-*trn*T, *atp*B-*rbc*L and *acc*D-*psa*I) and two single-low copy nuclear genes *CAMX* (Calmodulin) and ITS of 423 individuals from 23 populations, we found high genetic variation mainly existed between the populations (cpDNA: 89.80%, ITS: 84.55%, *CAMX*: 95.68%). Haplotypes in different river basins showed significant phylogeographical structure. The geographical distribution of haplotypes indicated that there is a high degree of genetic differentiation and this differentiation is associated with altitude discrepancy. BARRIER analysis detects a strong geographic barrier between the Nanpan River and Jinsha River. The MaxEnt result shows that the suitable distribution area was the largest in the LGM. The future climate warming will lead to the niche expansion for *H. lichiangensis* but will also cause fragmented distribution.

Conclusions: Our study highlighted the importance of altitude in explaining the genetic differentiation. The current phylogeographical pattern of *H. lichiangensis* may be shaped by long-term geographical isolation resulted from the uplifting of Himalaya, which gives rise to the barriers from the Hengduan Mountain or multiple river systems, and the vertical altitude discrepancies that both limited gene flow among regions. The Middle Jinsha River valley is most likely to be a main refuge for *H. lichiangensis* till now, and the glaciation retreat may account for the high endemism of plants in the dry-hot valleys of southwest China.

Background

The global climate fluctuations after the Quaternary [< 2 million years ago (Ma)] have resulted in repeated drastic environmental changes and profoundly shaped the current distributions and genetic structures of many plant and animal species in the Northern Hemisphere temperate zones [1]. A plenty of phylogeographic and biogeographic studies has emphasized the preponderant roles of these tectonic and climatic events for understanding the biogeographic history, diversification, and intraspecific genetic structure of many plant and animal taxa [2]. At the end of the Quaternary, the neotectonic movement inherited and developed by the Himalayan movement laid the foundation for the structure and characteristics of China's modern natural environment [3]. The Qinghai-Tibet Plateau (QTP), due to the size and height of the uplift in the late Pleistocene, produced significant effects on the surrounding

atmospheric circulation and surrounding areas, forming the modern monsoon circulation [4]. The modern monsoon circulation aggravated the degree of dryness and wetness in east and west. Simultaneously, the elevation of Hengduan Mountain-Yunnan Plateau topography and the river valleys (e.g. dry-hot valleys) also changed the distribution pattern of biological and natural zonality [3].

The Hengduan Mountain region, which locates in the eastern part of the Qinghai-Tibet Plateau, has long been considered as a refuge for the plants in the northern temperate during the Quaternary glacial period, and it has become an important source and radiation area for the plants in the northern temperate zone after the late glacial period [5]. Therefore, the existing distribution pattern of plant species in this region reflects the influence of plateau uplift and glacial period to some extent in the way of microevolution and macroevolution. With the uplift of Qinghai-Tibet Plateau and Yunnan-Guizhou Plateau since the Tertiary period, ridge-valley differentiated landform of this region has been formed by erosion of several large rivers, and then unique vegetation has evolved for the reason of the typical hot and dry climate [6]. The geographical location of the distribution of these valleys includes the Red River valley, Jinsha River valley, Salween valley, Mekong valley and Nanpan River valley in Yunnan and Sichuan [2]. These dry-hot valleys from Southwest China are dominated by drought-tolerant tropical flora and vegetation types, is also known as “Semi-savanna” [7]. Despite the harsh dry climate of the dry-hot valley in Southwest China, it harbors more than 1700 plant species, belonging to 752 genera and 165 families with most families are subtropical species and few are warm-temperate and tropical species. In particular, the high endemism (622 of 1707, ca. 37%) [8] of plant taxa in the dry-hot valley makes it a hypothetical refuge during the glacial period.

Understanding the origin, diversity and historical dynamics of the dry-hot valley endemic and endangered taxa can help us better unravel their evolutionary processes and manage the conservation. There are a couple of studies in the genetic structure and speciation of endemic and endangered plants taxa in the dry-hot valleys of Southwest China, such as *Trailliaedoxa gracilis* [9], *Leucomeris decora* and *Nouelia insignis* [10]. However, those cases are mostly focusing in a restricted region, and studies on taxa across various valleys with extensive distribution pattern are scanty. One example is the modern disjunctive distribution of *Terminalia franchetii* from the dry-hot valleys, which is associated to the patterns of cpDNA haplotype variation, resulting from vicariance caused by several historical river separation and capture events [11]. Another case study of *Sophora davidii* exemplified the utility of comparing chloroplast and nuclear DNA variability and suggested a major phylogeographic break in cpDNA within the riparian shrub *S. davidii* associated with the “Tanaka-Kaiyong Line” (TKL), and the complex geological and climatic changes in Hengduan Mountain area played a decisive role in the west-east differentiation of S. *davidii* [12]. These previous studies suggested geological historical events and biogeographical barriers had an indelible effect on genetic divergence and vicariant isolation of in Southwest China, particularly in the dry-hot valley, while comprehensive studies with multifactor involved are still limited in illuminating the temporal phylogeographical pattern and evolutionary process of the species assemblies of this region.

Himalrandia lichiangensis (W. W. Sm.) Tirveng. is a spineless perennial shrub of Rubiaceae, and is endemic to dry-hot valley in southwest China especially in Jinsha River. Our field survey indicates that the distribution range of *H. lichiangensis* is not confined to the basin of Jinsha River, but extends to the Red River and Nanpan River basin (Fig. 1). It mainly distributes on both sides of gullies at an altitude ranges from 1200 m to 2500 m, where the climate is rather dry and hot. Considering the extensive geographical distribution of *H. lichiangensis* in various basins, here we raise the following questions in this study. First, how is the distribution of *H. lichiangensis* in the past and whether the current distribution range and genetic structure of *H. lichiangensis* is affected by geological events in history. Second, whether there is distinct phylogeographical pattern among the populations of *H. lichiangensis* and if there is, what is accounting for it. Third, how will the distribution of *H. lichiangensis* shift in the future?

Results

Sequence characteristics, genetic diversity and differentiation

The aligned sequences lengths of the combined cpDNA, ITS and *CAMX* regions were 3448 bp, 643 bp and 854 bp, respectively. Among the 423 individuals (23 populations) surveyed, 19 cpDNA, 21 ITS and 15 *CAMX* haplotypes were identified, which have been deposited in GenBank (Table S1). Genetic diversity indices of total nucleotide (*Pi*) and haplotype diversity (*Hd*) for all populations were summarized in Table S2. The combined cpDNA showed the highest diversity indices in *Pi* and *Hd*, comparing with nuclear ITS and *CAMX* at the species level. Total genetic diversity (H_T=0.952, 0.785, 0.812 from cpDNA, ITS and *CAMX*, respectively) was higher than the average intrapopulation diversity (H_S=0.124, 0.197 and 0.053 from cpDNA, ITS and *CAMX*, respectively), resulting in high levels of genetic differentiation (G_{ST} = 0.925, 0.749, 0.934; N_{ST}=0.959, 0.842, 0.960, from cpDNA, ITS and *CAMX*, respectively, Table 1). The U tests showed that N_{ST} was significantly greater than G_{ST} (P = 0.006, 0.005, 0.044 for cpDNA, ITS and *CAMX*, respectively), implying that there is correspondence between haplotypes lineages and geographic distribution. The results of Mantel test also revealed the same pattern, namely, there is a significant positive correlation between genetic distance and geographical distance (cpDNA: r = 0.182, P < 0.05; ITS: r = 0.354, P < 0.05; *CAMX*: r = 0.331, P < 0.05), which indicated that the genetic pattern of this species was in accord with Isolation by Distance (IBD) (Figure S1).

Table 1
Genetic diversity, differentiation indices for the combined cpDNA and nDNA in this study

Markers	H_S	H_T	G_{ST}	N_{ST}
cpDNA	0.124 (0.0410)	0.952 (0.0225)	0.925 (0.0317)	0.959 (0.0228)
ITS	0.197 (0.0592)	0.785 (0.0493)	0.749 (0.0696)	0.842 (0.0562)
CAMX	0.053 (0.0337)	0.812 (0.0607)	0.934 (0.0398)	0.960 (0.0276)

H_T: total genetic diversity; H_S: average intrapopulation diversity; N_{ST} and G_{ST}: gene differentiation coefficient.

The AMOVA revealed that 89.80% of the genetic variation was presented among populations and 10.20% was within populations at the cpDNA level, consistent with the nDNA data, meaning that genetic variations existed predominantly among populations (Table 2). In addition, we detected high level of genetic differentiation (F_{ST} = 0.898, 0.846, 0.957 from cpDNA, ITS and *CAMX*, respectively). The results of the mismatch analysis for all populations displayed a multimodal distribution pattern (Figure S2) with non-significant positive values of SSD (Table 3), which indicates that the species has not undergone a recent population expansion. This conclusion is also supported by neutrality test, which yielded positive values in most results (Table 3).

Table 2
Analysis of molecular variance (AMOVA) based on cpDNA and nDNA haplotype frequencies for populations.

Markers	Source of variation	d.f.	Sum of squares	Variance components	Percentage of variation	F_{ST}	*N*m
cpDNA	Among populations	22	991.146	2.32600 Va	89.80%	0.898	0.029
	Within populations	400	110.750	0.26432 Vb	10.20%		
ITS	Among populations	22	1353.471	1.66622 Va	84.55%	0.846	0.046
	Within populations	823	326.900	0.39721 Vb	15.45%		
CAMX	Among populations	22	1035.059	1.22052 Va	95.68%	0.957	0.011
	Within populations	823	47.550	0.05516 Vb	4.32%		

F_{ST}: genetic differentiation; *N*m: gene flow

Table 3
Parameters of neutrality tests and mismatch analysis.(*P < 0.05, **P < 0.01)

Markers	Tajima's D	Fu's *Fs*	Raggedness	SSD
cpDNA	2.00446	3.232	0.0177	0.04772
ITS	2.61304*	-0.015	0.1357	0.01788
CAMX	0.82801	0.148	0.0391	0.00202
SSD: The variance of an observation of a point of difference with an expected value.				

Haplotype analyses

For the cpDNA haplotype distribution analysis, among the 19 detected haplotypes, 13 were exclusive for single populations (H3-7, H9-12, H16-19; see Table S2, Fig. 1), while three (H10, H11, H15) were present only among populations located in the Red River region (HT, LZ, XG). In contrast, the remaining haplotypes, H1 was the most frequent and occupied among all populations, showing a conspicuous disjunctive distribution pattern between the Jinsha River and southern Nanpan River systems. However, H8 was mainly found in Middle Jinsha River (NL, HP), Dadu River (LD) and the Red River (HT), it is noteworthy that LD is the only site found located in the Dadu River, which is the tributary of Lower Jinsha River. H2 is only distributed in the Pudu River basin, a tributary of the Jinsha River, which is closest to the Nanpan River. In addition, H13 is found only in the Middle Jinsha River (YG, JP, XY), so is H14. For the nuclear region *CAMX*, 15 haplotypes were detected (see Table S2, Fig. 2a). C2 was the most dominate haplotype (Jinsha River: CH, DL, EY, HL, HP, JP, SY. Red River: LZ, XG). Of the 15 haplotypes, 10 were private haplotypes (C3, C4, C6-C11, C14, C15), which mainly occurred in the Middle Jinsha River (JP, MD, WM, YG) and the Red River (HT). C1 distributed in the Nanpan River (XS, HD, AS), and the closest population (KD) also shares this haplotype. The remaining haplotypes (C5, C12 and C13) locate along the Jinsha River basin. For the ITS, a total of 21 haplotypes were detected (see Table S2, Fig. 2b). T1 is shared by three basins, including the the Red River (LZ, XG), Nanpan River (XS, AS, HD) and the Middle Jinsha River (HP, MD, SY, WM, XY, YG). T2 is widely distributed in Jinsha River (CH, DL, HL, JP, KD, MJ, SG, EY). Furthermore, a total of 11 private haplotypes (T4, T7, T9, T10, T11, T12, T14, T17, T18, T20, T21) were found, mainly distributed in the Middle Jinsha River (DL, HP, JZ, SY, WM) and the The Red River (HT, LZ). The rest of the haplotypes (T5, T6, T8, T13, T15, T16, T19) were shared by two populations, T3 was shared by five populations.

Network and phylogenetic analysis of haplotypes

Network analysis of the cpDNA haplotypes suggested that the 19 haplotypes formed two distinct monophyletic clades (clade1: H5, H6, H8, H10, H11, H16, H17; clade2: H1-H4, H7, H9, H12-H15, H18, H19) (Fig. 1). H1 is the haplotype with the most frequent occurrence and locates at the center of the reticular network tree. Phylogeny of chloroplast haplotypes based on Bayesian Inference (BI) method is consistent with the two groups defined by Network analysis (Fig. 3). Based on the network analysis of the *CAMX*

haplotypes (Fig. 2), the haplotype C2 which locates at the center appears to be the most frequent one. The HT population from the Red River basin occupied a private haplotype C3, which is closed to C2 with several mutant steps. The network analysis of ITS indicates T1 and T2 are the most two frequent haplotypes. Besides, it can be found that there are many private haplotypes between T2 and T1, and these haplotypes are basically displayed in the Middle Jinsha River.

STRUCTURE and BARRIER analyses

STRUCTURE analysis suggested the optimal value of K (ΔK) is two, namely, 19 populations were divided into two groups (Fig. 4), of which Clade II consisted of populations CH, HL, DL, KD, EY, JP, MJ, MJ and SG, the remained fifteen populations belong to Clade I. The T test shows that the elevation distribution of Group I and Group II was significantly correlated. And there is a corresponding relationship between the results of STRUCTURE and T test.

The results of BARRIER analysis show that there are two obvious isolation barrier with high bootstrap values (Fig. 5), one roughly locates between Dongyi River populations (MJ, EY) and Shuiluo River (NL), and the other barrier separates the Nanpan River populations (AS, XS) and Jinsha River populations (KD, CH). In order to infer the phylogenetic placement of *H. lichiangensis* in Rubiaceae and its divergent time, we reconstructed a Bayesian tree of Rubiaceae based on *rbc*L, showing the close relationship between *H. lichiangensis* and *Tarenna drummondii* (in the same genus as the outgroup *Tarenna depauperata* and *Tarenna attenuata.* Figure S3). BEAST results based on both cpDNA and nDNA datasets (Fig. 6) show that the divergence time of haplotypes. Estimates of the time of divergence suggest that the cpDNA haplotype diverged during the early Pliocene to Pleistocene (95%HPD: 21.3–33.3 Ma), suggesting that the infraspecific divergence in the glacial period. Results based on ITS and *CAMX* displayed similar divergent time. The BEAST results of *CAMX* show that 19 haplotypes clustered into two lineages, one includes C6-C10, and the remainder is another lineage characterized by C11 as an dominant haplotype. The haplotypes of ITS also constitute two lineages, one includes haplotypes T1, T3, T9, T11- T14, and the rest belong to another lineage.

Ecological niche modelling

The accuracy of MaxEnt model was tested by receiver operator characteristic (ROC), and the areas under receiver operator characteristic curves (AUC) value was greater than 0.980, indicating that the model had high stability and accuracy under the condition of a sample size of 23. The simulation results show that the current distribution area is well captured by the niche model, and most probable distribution area (> 0.8) is mainly from the middle reaches of Jinsha River to the upper reaches of the Red River (Fig. 7). Under the climatic condition of the Last Interglacial (LIG), the optimal distribution area was greatly reduced comparing with the current distribution area. During the Last Glacial Maximum (LGM), the suitable area expanded significantly, reaching the farthest north to Gansu, China. The most probable distribution area (> 0.8) mainly concentrated in the middle and lower basin of Jinsha River and Nanpan River. Under the future climatic conditions (in 2070s), the suitable distribution area *H. lichiangensis* will

shrink, accompanying by a large degree of habitat fragmentation. In addition, the potential distribution range of *H. lichiangensis* will expand significantly to the west and north.

Discussion

High genetic diversity of H. lichiangensis at the species level

High species level genetic diversity was detected within *H. lichiangensis* (cpDNA: H_T = 0.952, π = 0.00145, *H*d = 0.197; ITS: H_T = 0.785, π = 0.00568, *H*d = 0.761; *CAMX*: H_T = 0.812, π = 0.00268, *H*d = 0.754). This is in accordance with the case of *Trailliaedoxa gracilis*, another dry-hot valley species from Rubiaceae which showed comparable high levels of genetic diversity (cpDNA: H_T = 0.952, π = 0.00146, *H*d = 0.8311; nDNA: H_T = 0.966, π = 0.00466, *H*d = 0.9011) [13]. Life form and breeding system had highly significant influences on genetic diversity and its distribution [14]. *H. lichiangensis* is a perennial wind-pollinated shrub, and the berry fruit facilitates its long-distance dispersal, resulting its expected high genetic diversity. However, our results also suggest that there is extremely low genetic diversity within some populations (such as AS, HD, XS from the Nanpan River basin). The low genetic diversity of the three populations could be explained by species habitat fragmentation and genetic drift, in which few haplotypes were fixed because of the bottleneck effect [15].

High level of genetic differentiation accompanied by limited seed dispersal ability

Geographical isolation, mutation, turbulent environmental factors and isolation of gene flow in plant populations can give rise to differences in the genetic structure of the populations, and eventually lead to population differentiation [16]. Our AMOVA results *H. lichiangensis* reveals that a large proportion of genetic variation exists among populations (cpDNA: 89.90%, ITS: 84.55%, *CAMX*: 95.68%), leading to a high level of genetic differentiation (F_{ST}=0.898, 0.846, 0.957 from cpDNA, ITS and *CAMX*, respectively). The fragmentation of habitats leads to fragmented ancestral populations; and with a single genetic background, the effect of genetic drift in a small population is more significant [17]. Generally, species with fragmented habitat tends to have lower population genetic diversity within populations and high genetic differentiation among populations. *H. lichiangensis* mainly grows in the dry hot valley or sparse forest, where the habitat in distribution area is highly fragmented. Of the 23 populations studied, nine contained only one haplotype (AS, HD, KD, LD, MJ, NL, SG, XG, XS), both cpDNA and nDNA, i.e. no haplotype diversity within the population, which further explained the bottleneck effect or genetic drift caused by small populations [18]. Based on Wright's calculation formula in gene flow $Nm = (1-F_{ST})/4F_{ST}$ [19], here we deduced the gene flow between population pairs of *H. lichiangensis*. The value of gene flow obtained by this method is explained as follows: when $Nm < 1$, less than one individual migrates between populations in each generation on average, and the population is expected to continue to be

differentiated due to the intense influence of genetic drift; when $Nm > 1$, i.e. gene flow can prevent genetic differentiation between populations caused by genetic drift [20]. The gene flow estimated by F_{ST} values between populations is shown in Table 2 (cpDNA: 0.029, ITS: 0.046, *CAMX*: 0.011). Low gene flow levels indicate infrequent contacts between populations. In general, species whose seeds are dispersed by gravity have greater genetic differentiation among populations; species whose seeds are dispersed by wind, however, have less differentiation among populations due to the longer distances [21]. The ripe fruit of *H. lichiangensis* is black berry, so it is not possible to spread seeds by wind. The seed dispersal may be possibly driven by gravity and water flow if bird or other animal mediated long-distance dispersal were not taken into consideration. The barrier effect of high mountain valley directly affects the seed dispersal range, so the limited seed dispersal may be the reason for the large genetic differentiation of *H. lichiangensis* and obvious phylogeographical structure among its populations in different areas.

The most ancient haplotypes are more likely to locat at the center of the network and be geographically widespread, whereas the most recent haplotypes could be at the tips of the network and be geographically restricted [22]. As a corollary, it is possible that haplotype H1 stands for ancient haplotype from the network analysis based on the cpDNA haplotypes. In addition, for the *CAMX* haplotypes, there was no genetic differentiation among the populations in the Nanpan River, and the haplotype C1 was shared with the nearest Jinsha River population KD. Similarly, the haplotype C5 was shared by LD, YG and WM, and this may be the result of long-distance propagation through animals or rivers. It is obvious that the mesh shows many closed loops in the ITS network, which may be caused by the absence of intermediate haplotypes likely due to incomplete sampling [23].

Allopatric speciation and ecological adaptation

Haplotype distribution diagram and network were constructed based on cpDNA and nDNA. The results suggested that *H. lichiangensis* could be divided into distinct lineages based on different drainage basin. BARRIER analysis detects a strong geographic barrier between the Nanpan River and Jinsha River (Fig. 5). *H. lichiangensis* mainly distributes in the dry-hot valleys of Hengduan Mountains region. The formation of Hengduan mountains is closely related to the uplift of Qinghai-Tibet Plateau caused by the collision between the Indian and the Eurasian plate. It is the product of the lateral extrusion after the collision and extrusion of the plate [24]. Based on the divergence between *H. lichiangensis* and its closest sister, we estimated that the time of lineage divergences were from fifteen to one MYA (Fig. 6), which was consistent with the time of rapid uplifting of Qinghai-Tibet Plateau and the formation time of East Asian monsoon [25]. We speculated that the *H. lichiangensis* may continuously distributed widely in this area at that time, until in the Miocene period (10 – 8 MYA), with the rapid uplifting of the Qinghai-Tibet Plateau and the orogeny of Hengduan Mountains which blocks the gene flow among populations, resulting in isolation, independent evolution and development of lineages in fragmented distribution regions. Since its favor of valley habitat, the barrier of rivers should be crucial in the process of differentiation of *H. lichiangensis*.

In addition, we also find that the genetic differentiation is associated with the altitude gradient [26]. Climate and topography are among the most fundamental drivers of plant diversity [27]. We deduce that

the species was initially widespread in this area before the rapid uplift of Himalaya, when gene flow could be still frequent among populations in a similar altitude context. With the formation of Hengduan Mountains, gradient elevation differences occurred among populations, and river erosion further hindered the gene flow between habitats in contrasting altitude elevations, which eventually resulted in the genetic differentiation [6]. Taken together, the spatial distribution of genetic diversity reflects a potentially adaptive differentiation between low- and high-altitude populations. It may resemble an interaction between adaptation to the local microhabitat and demographic history influenced by historical glaciation cycles, recent seed dispersal and genetic drift in local populations [28].

Similar patterns have been found in other groups of organisms in the Hengduan Moutain region. Gao et al. investigated the genetic distribution pattern of *Taxus wallichiana* and concluded that the barrier of the Nu Mountains caused its allopatric speciation [29]. The phylogeographical study of *Sinopodophyllum hexandrum* also reveal that the barrier of high mountain valleys formed by the uplift of Qinghai-Tibet Plateau led to the differentiation of the two lineages [30]. To sum up, allopatric speciation caused by uplift of the Qinghai-Tibet Plateau could be the major force in driving speciation and diversification of the Qinghai-Tibet Plateau and its adjacent areas, which may be one of the important factors contributing to the high biodiversity of the region [31].

Prediction of potential distribution and historical changes in four periods

The predicted potential current distribution range is larger than the actual distribution range, for instance, the Yarlung Zangbo River and The Mekong River also show the existence of suitable distribution area. According to the prediction of the suitable distribution area for each period, LGM has the largest potential area (Fig. 10). It seems low temperature in the glacial period does not cause the contraction of distribution areas, but provides conditions for expansion. During the Quaternary glaciation, high latitude species were affected by the spread of large ice sheets, which fragmented the geographical distribution of many species [32]. In China with relatively low latitude, the complex terrain and mountain barriers prevented the south of China from being covered by large ice sheets, making it one of the important refuges for the southward retreat of most of the Tertiary relic gymnosperms of East Asia during the Quaternary glacial period [33]. Therefore, the distribution area during the LGM period was less affected by the glacial period. The suitable distribution area shared by the species at different period tend to be refuge for the species [34]. Our ENM prediction demonstrates that the major distribution area of *H. lichiangensis* is relatively stable from past to future (except in LGM), mainly occurs in the midstream of Jinsha River and the upper reaches of the Red River. However, actions should be taken before the habitat fragmentation of *H. lichiangensis* in 2070 as predicted.

Glacial refuge and post-interglacial migration

Regions with high genetic diversity may indicate long-term survival of populations that have had a longer evolutionary history than populations that expanded after the glacial, which is often thought of as a possible refuge for plants [35]. The results showed that both nDNA and cpDNA had high genetic diversity

and more endemic haplotypes in the middle reaches of Jinsha River, so this area was likely to be a glacial refuge. Comps et al. proposed that there was no positive correlation between genetic diversity and refuge, and it was inaccurate to predict refuge regions based on the level of genetic diversity [36]. Apparently, populations located in marginal distribution zones (LD, AS, HD, XS) have significantly reduced genetic diversity, most likely as a result of refuge population migration. Studies have shown that many species whose refuge are located on the eastern edge of the Tibetan Plateau have undergone a similar expansion process after LGM (Last Glacial Maximum) such as *Pedicularis longiflora* which indicated the species expansion from the eastern fringe of the refuge to the plateau and a subsequent continuous founder effect, which significantly reduced the population diversity on the plateau, especially in the west [37].

Conclusions

We found high genetic diversity among populations at the species level in *H. lichiangensis* with no recent expansion detected, and its current distribution pattern may be caused by long-term geographical isolation. It is worth noting that the current genetic structure is closely related to the elevation gradient, which reflects the influence of the complex topographical structure in this area on the genetic differentiation. Since the obvious impeding effect on the gene flow by different rivers system, we also found significant phylogeographical structure of *H. lichiangensis* in different basin. The past distribution area of *H. lichiangensis* in the LGM was the largest, showing a trend of range expansion during the ice age and contraction after the glacial epoch. Besides climate warming in the coming 50 years will lead to a large decrease in the area suitable for *H. lichiangensis*, which offers imperative thinking for niche conservation and ecological restoration in dry-hot valley areas of Southwest China. The influence of geological events on the plant distribution in the dry-hot valley area needs to be extended to more plant groups in order to find a regular evolutionary model.

Methods

Field sampling

During the field survey in the dry hot valley of southwest China, we collected a total of 423 individuals from 23 localities almost covering the entire range of the species (Table S2). Each individual from the population was randomly sampled with a distance ≥ 5 m in the field. We chose 20 individuals from each population for genotyping, with three populations as exception where insufficient individuals can be found in those sites. Young and green leaf materials were stored with silica gel for DNA extraction. We designated two *Tarenna* species (*Tarenna attenuata* and *Tarenna depauperata*) as outgroup, and these two taxa were sampled from cultivated materials kindly provided by the Xishuangbanna Tropical Botanical Garden, Mengla, Yunnan, China.

DNA Extraction, PCR Amplification, and DNA Sequencing

Genomic DNA was extracted from the silica-dried leaves using the CTAB method [38]. Four chloroplast DNA regions were amplified and sequenced: *trn*D-*psb*M, *trn*D-*trn*T, *acc*D-*psa*I, *atp*B-*rbc*L, using the primers

described by Shaw et al [39, 40]. Besides, we amplified and sequenced the nuclear loci *CAMX* [41] and ITS4-ITS5 region [42] for all samples. PCR [43] and sequencing protocols were followed by the previous studies in which those primers were described.

Genetic diversity, genetic differentiation and haplotype network

A congruency test for the four combined cpDNA regions used in this study showed a significant rate of homogeneity ($P > 0.5$) by PAUP version 4.0b10 [44], suggesting a high degree of homogeneity of the cpDNA regions. Therefore, all cpDNA sequences were combined in the following analyses. Sequences were aligned using CLUSTAL X version 1.83 [45] and double examined manually. We calculated average within-population haplotype diversity (H_S), total diversity (H_T), the level of population differentiation (G_{ST}) as well as the genetic differentiation (F_{ST}) at the species level. To incorporate the relationships between haplotypes, an estimate of population subdivision for phylogenetically ordered alleles (N_{ST}) was obtained, comparing the values of N_{ST} and G_{ST} [46]. A significant higher N_{ST} than G_{ST} usually indicates the presence of phylogeographic structure. All these parameters were calculated using the program Permut ver. 1.0 [47]. We used Arlequin version 3.1 [48] to conduct the analysis of molecular variance (AMOVA) to estimate genetic variations within and among populations [49]. To test whether has undergone recent demographic population expansion events, we calculated Tajima's *D* [50] and Fu's *F*s [51] of each population and all populations using the program DNASP [52]. We also plotted the mismatch distribution as the observed number of differences between pairs of haplotypes using DNASP. These neutrality test statistics are increasingly accepted, which are meritorious in detecting departures from population size equilibrium caused by population expansions or bottlenecks [53].

Genealogical relationships among haplotypes were inferred from an unrooted statistical parsimony haplotype network as estimated by NETWORK 4.2 [54], with 95% most parsimonious connection. Mutation and gap (indel) were both treated equally as one step (a historical gap event) in the network analysis, and the gaps are independent from each other [55]. The geographical distribution of haplotypes and sampling localities are plotted in Arcgis 10.5 (https://developers.arcgis.com). Phylogenetic relationship of cpDNA and nDNA haplotypes were inferred using Bayesian methods implemented in MrBayes, version 3.1.2 [56]. The best substitution models of each analysis were decided by jModelTest 2.1 before the phylogenetic analyses [57].

STRUCTURE and BARRIER analyses

We conducted Bayesian clustering analysis of population structure based on the combined nDNA loci using the program STRUCTURE, version 2.2 [58]. Ten independent runs were performed for each set, with values of K ranging from 1 to 10, with a burn-in of 10^5 iterations and 10^5 subsequent MCMC steps. The best-fit number of grouping was evaluated using ΔK by STRUCTURE HARVESTER, version 0.6.8 [59]. We also estimated the haplotype divergence time of *H. lichiangensis* based on different data set in BEAST version 1.8.4 [60]. Before the haplotype divergence time inference, we inferred the systematic position of *H. lichiangensis* in Rubiaceae by using *rbc*L gene. Based on relaxed molecular clock, we further calibrated

the common ancestors [61] of *H. lichiangensis* and *Tarenna drummondii* [62] as diverging at about 27.3 Ma (95%HPD: 21.3–33.3 Ma) according to previous molecular dating study [63]. In addition, in order to test the significance of altitude differences among 23 populations, we grouped the populations according to the result of STRUCTRE and performed T test significance analysis of the altitude information of 23 populations was performed by T test [64] of different groups in theby R package ggsignif [65]. In order to display the impeding influence of physical barriers (river system) to gene flow, BARRIER 2.2 [66] was used to detect whether there were significant geographic isolation barriers between different populations. We used MICROSATELLITE ANALYSER 4.05 (MSA) [67] to acquire Nei's genetic distance (Da) [68] between populations matrix, and 1000 repetitions were run for the significance test of each potential barrier.

Ecological niche modelling

In order to simulate the potential distribution of *H. lichiangensis* in the past, current and future, we reestablished its distribution ranges in four periods (Last Inter Glacial, LIG; Last Glacial Maximum, LGM; current and future) using 23 presence records by niche modeling based on 19 bio-climatic factors [69]. The maximum entropy model (MaxEnt) [70] and ArcGis 10.5 (https://developers.arcgis.com) were used to predict the suitable ecological region [71]. Loading distribution point data (.csv format file) and environmental data set into MaxEnt software, and set operation parameters: randomly select 30% distribution points as test data, and the rest data as training data, with the maximum number of iterations being 500, and set other parameters as default values [71].

Abbreviations

cpDNA: Chloroplast DNA; nDNA: Nuclear DNA; *CAMX*: Calmodulin; ITS: Internal Transcribed Spacers; ML: Maximum Likelihood; BI: Bayesian Inference; NJ: Neighbor-joining; MCMC: Markov Chain Monte Carlo; BS: Bootstrap.

Declarations

Ethics approval and consent to participate

Not applicable.

Consent for publication

Not applicable.

Availability of data and materials

The analyzed sequences are publicly available and were downloaded from the Genebank (MW222416-MW222467, MW264453-MW264480). The plant materials are available from the corresponding authors on reasonable request.

Competing interest

The authors declare that they have no competing interests.

Funding

This study is funded and supported by the National Key Research and Development Program of China (2017YF0505200) to X. Gong, and the Light of West China Program (Y8246811W1) of the Chinese Academic of Sciences to J. Liu.

Authors’ contributions

Yaomei Qiao collected research materials, extracted DNA, analyzed entire data, conducted the molecular genetic studies and wrote the manuscript. Xun Gong and Jian Liu designed the study, collected research materials and drafted the manuscript. All authors read and approved the final manuscript.

Acknowledgements

Not applicable.

Authors' information

[1] CAS Key Laboratory for Plant Diversity and Biogeography of East Asia, Kunming Institute of Botany, Chinese Academy of Sciences, Kunming, Yunnan, China

[2] Key Laboratory of Economic Plants and Biotechnology, Kunming Institute of Botany, Chinese Academy of Sciences, Kunming, Yunnan, China

References

1. Qiu YX, Fu CX, Comes HP. Plant molecular phylogeography in China and adjacent regions:Tracing the genetic imprints of Quaternary climate and environmental change in the world's most diverse temperate flora. Mol Phylogenet Evol. 2011;59:244-225.

2. Hickerson MJ, Carstens BC, Cavender-Bares J. Phylogeography's past, present, and future: 10 years after Avise, 2000. Mol Phylogenet Evol. 2010;54:301-291.
3. He YB, Lu PZ, Zhu T. Causes for the formation of dry-hot valleys in Hengduan Mountain-Yunnan Plateau. Resour Sci. 2000;05:71-74.
4. Chi X, Zhang F, Gao Q, Xing R, Chen S. Genetic structure and Eco-Geographical differentiation of *Lancea tibetica* in the Qinghai-Tibetan Plateau. Genes. 2019;10:2.
5. Wang HS. The nature of China□s Flora and the relationships between its different element. Acta Botanica Yunnanica. 2000;02:126-119.
6. Harrison S, Noss, R. Endemism hotspots are linked to stable climatic refugia. Anna Bot. 2017;119:1247.
7. Liu Y, Zhu XX, Shen ZH, Sun H. Flora compositions and spatial differentiations of vegetation in dry valleys of southwest China. Biodiversity. 2016;24:377-367.
8. Ou XK, Jin ZZ. Preliminary study on floristic and ecological diversity in dry-hot valley of Jinsha River. J Wuhan Bot Res. 1996;04:322-318.
9. Jia J, Zeng Lq, Gong X. High genetic diversity and population differentiation in the critically endangered plant species *Trailliaedoxa gracilis* (Rubiaceae). Plant Mol Biol Rep. 2016;34:12-1.
10. Zhao YJ, Gong X. Genetic divergence and phylogeographic history of two closely related species (*Leucomeris decora* and *Nouelia insignis*) across the 'Tanaka Line' in Southwest China. BMC Evol Biol. 2015;15:134.
11. Zhang TC, Comes HP, Sun H. Chloroplast phylogeography of *Terminalia franchetii* (Combretaceae) from the eastern Sino-Himalayan region and its correlation with historical river capture events. Mol Phylogenet Evol. 2011;60:12-1.
12. Fan DM, Yue JP, Nie ZL, Li ZM, Comes HP, Sun H. Phylogeography of *Sophora davidii* (Leguminosae) across the 'Tanaka-Kaiyong Line', an important phytogeographic boundary in Southwest China. Mol Ecol. 2013;22:4288-4270.
13. Jia J. Conservation genetics of *Munronia delavayi* and *Trailliaedoxa gracilis*, endemic species in dry valleys, south-western China. Kunming Institute of Botany, Chinese Academy of Sciences. 2014.
14. Hamrick JL, Godt MJW. Effects of life history traits on genetic diversity in plant species. Phil Trans R Soc Lond B. 1996;351:1298-1291.
15. Allendorf FW. Isolation, gene flow, and genetic differentiation among populations. In: Schonewald-Cox, CM, SM Chambers, B MacBryde, WL Thomas, editors. Genetics and conservation: a reference for managing wild animal and plant populations. Menlo Park: Benjamin/Cummings; 1983.p.51-65.
16. Jacquemyn H, Honnay O, Galbusera P, Roldán in Uiz I. Genetic structure of the forest herb *Primula elatior* in a changing landscape. Mol Ecol. 2010;13:219-211.
17. Tsaliki M, Diekmann M. Effects of habitat fragmentation and soil quality on reproduction in two heathland Genista species. Plant Biol. 2010;12:629-622.

18. Birky CW, Fuerst P, Maruyama T. Organelle gene diversity under migration, mutation, and drift: Equilibrium expectations, approach to equilibrium, effects of heteroplasmic cells, and comparison to nuclear genes. Genetics. 1989;121:627-613.
19. Wright S. Evolution in Mendelian populations. Bull Math Biol. 1931;16:159-97.
20. Slatkin M. Gene flow in natural-populations. Annu Rev Ecol Syst. 1985;16:430-393.
21. Wang XR, Szmidt AE. Molecular markers in population genetics of forest trees. Scand J Forest Res. 2001;16:220-199.
22. Schaal BA, Hayworth DA, Olsen, KM. Phylogeographic studies in plants: problems and prospects. Mol Ecol. 1998;7:474-465.
23. Mardulyn P. Phylogeography of the Vosges mountains populations of *Gonioctena pallida* (Coleoptera: Chrysomelidae): a nested clade analysis of mitochondrial DNA haplotypes. Mol Ecol. 2001;10:1763-1751.
24. Coleman M, Hodges K. Evidence for Tibetan Plateau uplift before 14-Mya ago from a New Minimum Age for East-west Extension. Nature. 1995;374:52-49.
25. An ZS, Kutzbach JE, Prell WL, Porter SC. Evolution of asian monsoons and phased uplift of the Himalayan Tibetan Plateau since Late Miocene Times. Nature. 2001;411:66-62.
26. Sean GB, Yvonne P, Ary AH. Effect of altitude on the genetic structure of an Alpine grass, Poa hiemata. Ann Bot. 2009;103:899-885.
27. Irl S DH, Harter EV, Steinbauer MJ, Gallego PD, Maria Fernandez-Palacios Jose, Jentsch A, Carl B. Climate vs. topography-spatial patterns of plant species diversity and endemism on a high-elevation island. J Ecol. 2015;103:1633-1621.
28. Torsten G, Christian L, Ivan B, Karl JS. Genomic and phenotypic differentiation of Arabidopsis thaliana along altitudinal gradients in the North Italian Alps. Mol Ecol. 2016;25:3592-3574.
29. Gao LM, Moeller M, Zhang XM, Hollingsworth ML, Liu J, Mill RR, Gibby M, Li DZ. High variation and strong phylogeographic pattern among cpDNA haplotypes in Taxus wallichiana (Taxaceae) in China and North Vietnam. Mol Ecol. 2007;16:4684-98.
30. Li Y, Zhai S-N, Qiu Y-X, Guo Y-P, Ge X-J, Comes HP. Glacial survival east and west of the 'Mekong-Salween Divide' in the Himalaya-Hengduan Mountains region as revealed by AFLPs and cpDNA sequence variation in *Sinopodophyllum hexandrum* (Berberidaceae). Mol Phylogenet Evol. 2011;59:424-412.
31. Xu T, Abbott RJ, Milne RI, Mao K, Du FK, Wu G, Ciren Z, Miehe G, Liu J. Phylogeography and allopatric divergence of cypress species (Cupressus L.) in the Qinghai-Tibetan Plateau and adjacent regions. BMC Evol Biol. 2010;10:194.
32. Wang Q, Abbott RJ, Yu QS, Lin K, Liu JQ. Pleistocene climate change and the origin of two desert plant species, *Pugionium cornutum* and *Pugioniumdolabratum* (Brassicaceae), in northwest China. New Phytol. 2013;199:277-87.

33. Kusky T, Guo L, Xiang S, Guo X, Xu X. A critical examination of evidence for a Quaternary glaciation in Mt. Laoshan, Eastern China. J Asian Earth Sci. 2011;40:416-403.
34. Tang CQ, Matsui T, Ohashi H. Identifying long-term stable refugia for relict plant species in East Asia. Nat Commun. 2018;9:4488.
35. Taberlet P, Fumagalli L, Wust-Saucy AG, Cosson JF. Comparative phylogeography and postglacial colonization routes in Europe. Mol Ecol. 1998;7:464-453.
36. Comps B, Gomory D, Letouzey J, Thiebaut B, Petit RJ. Diverging trends between heterozygosity and allelic richness during postglacial colonization in the European beech. Genetics. 2001;157:397-389.
37. Yang F-S, Li Y-F, Ding X, Wang X-Q. Extensive population expansion of *Pedicularis longiflora* (Orobanchaceae) on the Qinghai-Tibetan Plateau and its correlation with the Quaternary climate change. Mol Ecol. 2008;17:5145-5135.
38. Doyle J, DNA protocols for plant-CTAB total DNA isolation. In: GM Hewitt, A Johnston, editors. Molecular techniques in taxonomy. Berlin:Springer; 1991.p.283-293.
39. Shaw J, Lickey EB, Beck JT, Farmer SB, Liu W, Miller J, Siripun KC, Winder CT, Schilling EE, Small RL. The tortoise and the hare II: relative utility of 21 noncoding chloroplast DNA sequences for phylogenetic analysis. Am J Bot. 2005;92:166-142.
40. Joey Shaw EBL, Edward E. Schilling, Small RL. Comparison of whole chloroplast genome sequences to choose noncoding regions for phylogenetic studies in angiosperms: the tortoise and the hare III. Am J Bot. 2007;94:288-275.
41. Strand AE, Mack JL, Milligan BG. Nuclear DNA-based markers for plant evolutionary biology. Mol Ecol. 2010;6:118-113.
42. White TJ, Bruns T, Lee S, Taylor J. Amplification and direct sequencing of fungal ribosomal RNA genes for phylogenetics. In: Innis MA, Gelfand DH, Sninsky JJ, White TJ, editor. PCR Protocols. 1990.p.322-315.
43. Clark AG. Inference of haplotypes from PCR-amplified samples of diploid populations. Mol Biol Evol. 1990;7:122-111.
44. Swofford DL. PAUP*4.0: phylogenetic analysis using parsimony. (* and Other Methods). Sunderland: Sinauer Associates, 2003.
45. Thompson JD, Gibson TJ, Frédéric P, Franois J, Higgins DG. The CLUSTAL_X windows interface: flexible strategies for multiple sequence alignment aided by quality analysis tools. Nucleic Acids Res. 1997;25:4882-4876.
46. Heuertz M, Carnevale S, Fineschi S, Sebastiani F, Hausman JF, Paule L. Chloroplast DNA phylogeography of European ashes. Mol Ecol. 2006;15:2131-40.
47. Pon S, Petit RJ. Measuring and testing genetic differentiation with ordered versus unordered addeles. Genetics. 1996;144:1245-1237
48. Excoffier L, Laval G, Schneider S. Arlequin (version 3.0): An integrated software package for population genetics data analysis. Evol Bioinform. 2005;1:50-47.

49. Excoffier L, Smouse PE, Quattro JM. Analysis of molecular variance inferred from metric distances among DNA haplotypes: application to human mitochondrial DNA restriction data. Genetics. 1992;131:491-479.
50. Tajima F. The amount of DNA polymorphism maintained in a finite population when the neutral mutation rate varies among sites. Genetics. 1996;143:1457-65.
51. Fu X, Yun. Statistical tests of neutrality of mutations against population growth, hitchhiking and background selection. Genetics. 1997;147:915-25.
52. Rozas J, Rozas R, Sánchez-DelBarrio JC, Messeguer X. DnaSP, DNA polymorphism analyses by the coalescent and other methods. Bioinformatics. 2003;19:2497-2496.
53. Korneliussen TS, Moltke I, Albrechtsen A, Nielsen R. Calculation of Tajima's D and other neutrality test statistics from low depth next-generation sequencing data. BMC Bioinformatics. 2013;14:289.
54. Bandelt HJ, Forster P, Rohl A. Median-joining networks for inferring intraspecific phylogenies. Mol Biol Evol. 1999;16:48-37.
55. Caicedo AL, Schaal BA. Population structure and phylogeography of *Solanum pimpinellifolium* inferred from a nuclear gene. Mol Ecol. 2010;13:1882-1871.
56. Ronquist F, Huelsenbeck JP. MrBayes 3: Bayesian phylogenetic inference under mixed models. Bioinformatics. 2003;19:1574-1572.
57. David P. jModelTest: Phylogenetic model averaging. Mol Biol Evol. 2008;7:7.
58. Pritchard JK, Stephens M. Inference of population structure using multilocus genotype data. Genetics. 2000;155:945–59.
59. Earl DA, Vonholdt BM. STRUCTURE HARVESTER: a website and program for visualizing STRUCTURE output and implementing the Evanno method. Conserv Genet Resour. 2012;4:361-359.
60. Drummond AJ, Rambaut A. BEAST: Bayesian evolutionary analysis by sampling trees. BMC Evol Biol. 2007;7:214.
61. Bender MA, Farach-Colton M. The LCA problem revisited. In: G Goos, J Hartmanis, J van Leeuwen. Latin American Symposium on Theoretical Informatics. Springer:Berlin; 2000.p.88-94
62. Bremer B, Eriksson T. Time tree of Rubiaceae: phylogeny and dating the Family, Subfamily, and Tribes. Int J Plant Sci. 2009;170:793-766.
63. Bremer B, Andreasen K, Olsson D. Subfamilial and tribal relationships in the Rubiaceae based on *rbc*L sequence data. Ann Mo Bot Gard. 1995;82:397-383.
64. Niu K, Chen Y. T-test principle and Comparative Application in Hypothesis Testing. Industry and Technology Torum. 2019;18:51-50.
65. Lan Y, He X, Zhu XM, Zhang YJ. Application of R language graphics in biological research. Journal of East China Normal University (Natural Science). 2019;1:144-124.
66. Manni F, Guerard E, Heyer E. Geographic patterns of (genetic, morphologic, linguistic) variation: How barriers can be detected by using Monmonier's algorithm. Hum Biol. 2004;76:190-173.

67. Dieringer D, Schlotterer C. MICROSATELITE ANALYSER (MSA): a platform independent analysis tool for large microsatellite data sets. Mol Ecol Notes. 2003;31:169-167.
68. Nei MF, Tajima F, Tateno Y. Accuracy of estimated phylogenetic trees from molecular data - II. Gene frequency data. J Mol Evol. 1983;19:170-153.
69. Zhang W-X, Kou Y-H, Zhang L, Zeng W-D, Zhang Z-Y. Suitable distribution of endangered species *Pseudotaxus chienii* (Cheng) Cheng (Taxaceae) in five periods using niche modeling. Chin J Ecol. 2020;39:613-600.
70. Elith J, Graham CH, Anderson RP, Dudik M, Ferrier S, Guisan A, Hijmans RJ, Huettmann F, Leathwick JR, Lehmann A. Novel methods improve prediction of species' distributions from occurrence data. Ecography. 2006;29:151-129.
71. Hernandez PA, Graham CH, Master LL, Albert DL. The effect of sample size and species characteristics on performance of different species distribution modeling methods. Ecography 2006, 29(5):785-773.

Figures

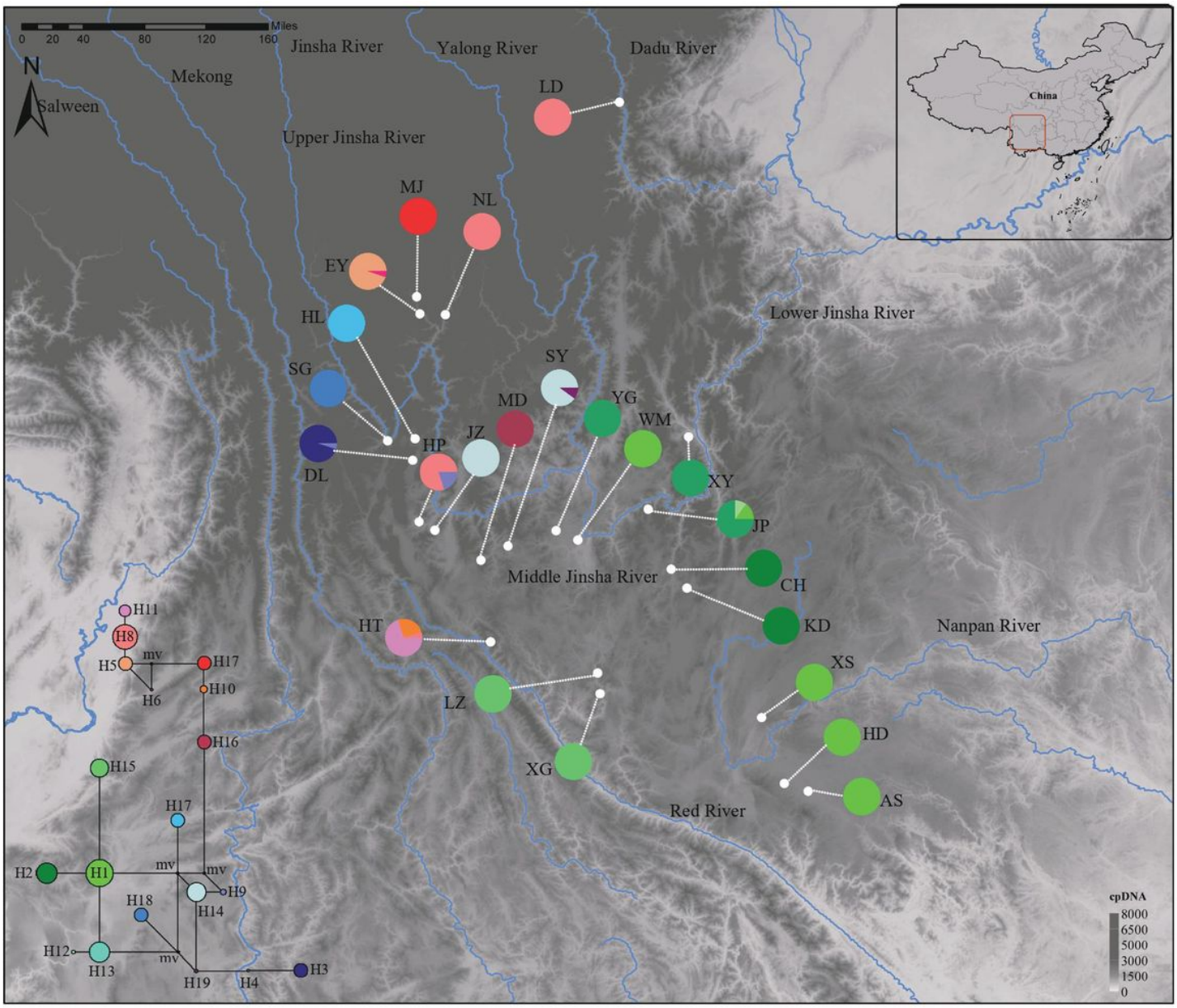

Figure 1

Geographical distribution of cpDNA haplotypes in 23 populations of H. lichiangensis. Population names are the same as for Table S1. Frequency of cpDNA haplotypes in each population is indicated by the pie diagrams. The lower left corner were haplotype network analysis. The size of each circle is proportional to the haplotypes frequency. Each solid line represents one mutational step that interconnects two haplotypes. The small bold circles indicated inferred intermediate haplotypes not detected in this investgation. Note: The designations employed and the presentation of the material on this map do not imply the expression of any opinion whatsoever on the part of Research Square concerning the legal status of any country, territory, city or area or of its authorities, or concerning the delimitation of its frontiers or boundaries. This map has been provided by the authors.

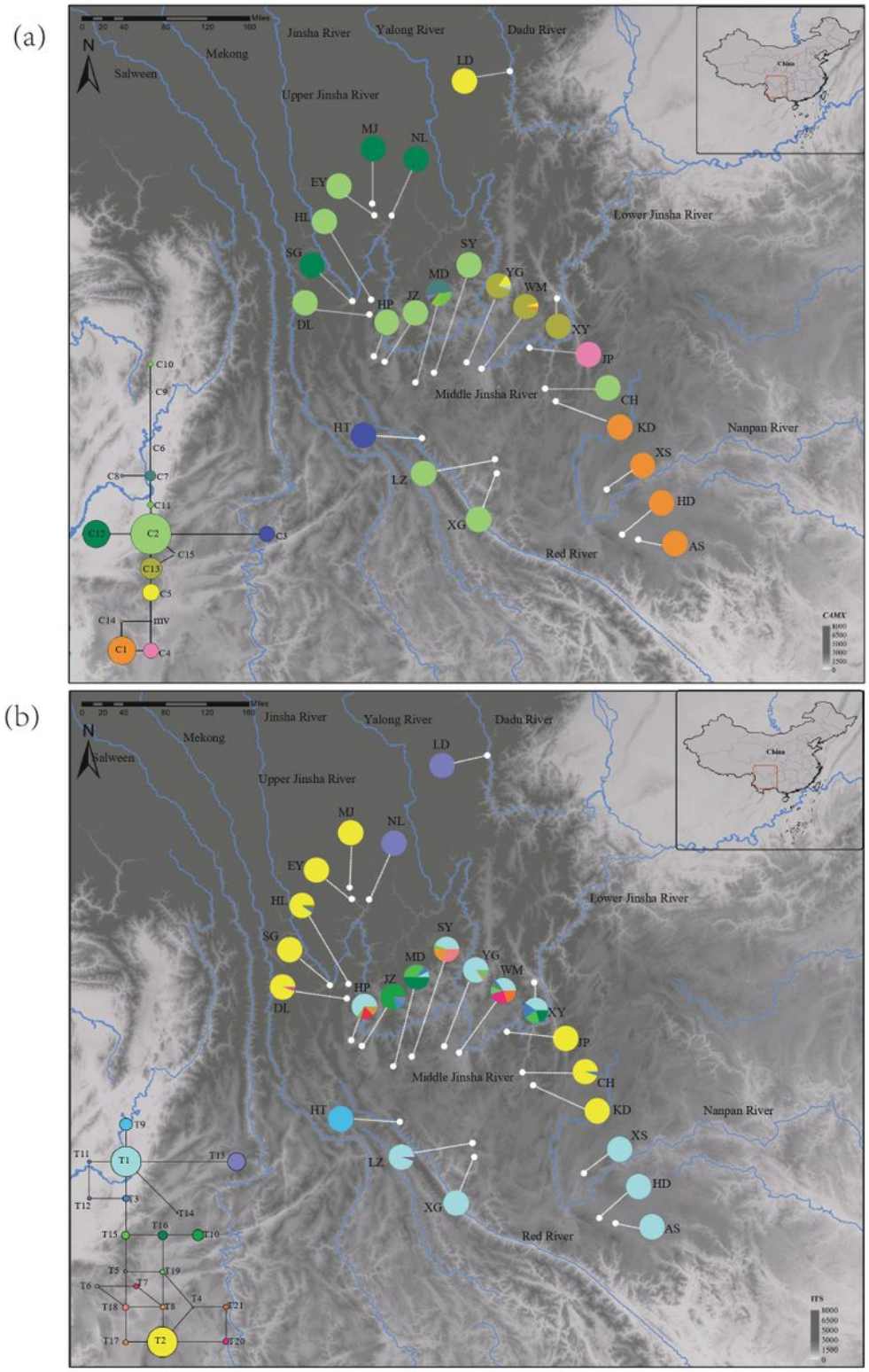

Figure 2

Geographical distribution of CAMX haplotypes (a), and ITS haplotypes (b) in 23 populations of H. lichiangensis. Population names are the same as for Table S1. Frequency haplotypes in each population is indicated by the pie diagrams. The lower left corner were haplotype network analysis. The size of each circle is proportional to the haplotypes frequency. Each solid line represents one mutational step that interconnects two haplotypes. The small bold circles indicated inferred intermediate haplotypes not

detected in this investgation. Note: The designations employed and the presentation of the material on this map do not imply the expression of any opinion whatsoever on the part of Research Square concerning the legal status of any country, territory, city or area or of its authorities, or concerning the delimitation of its frontiers or boundaries. This map has been provided by the authors.

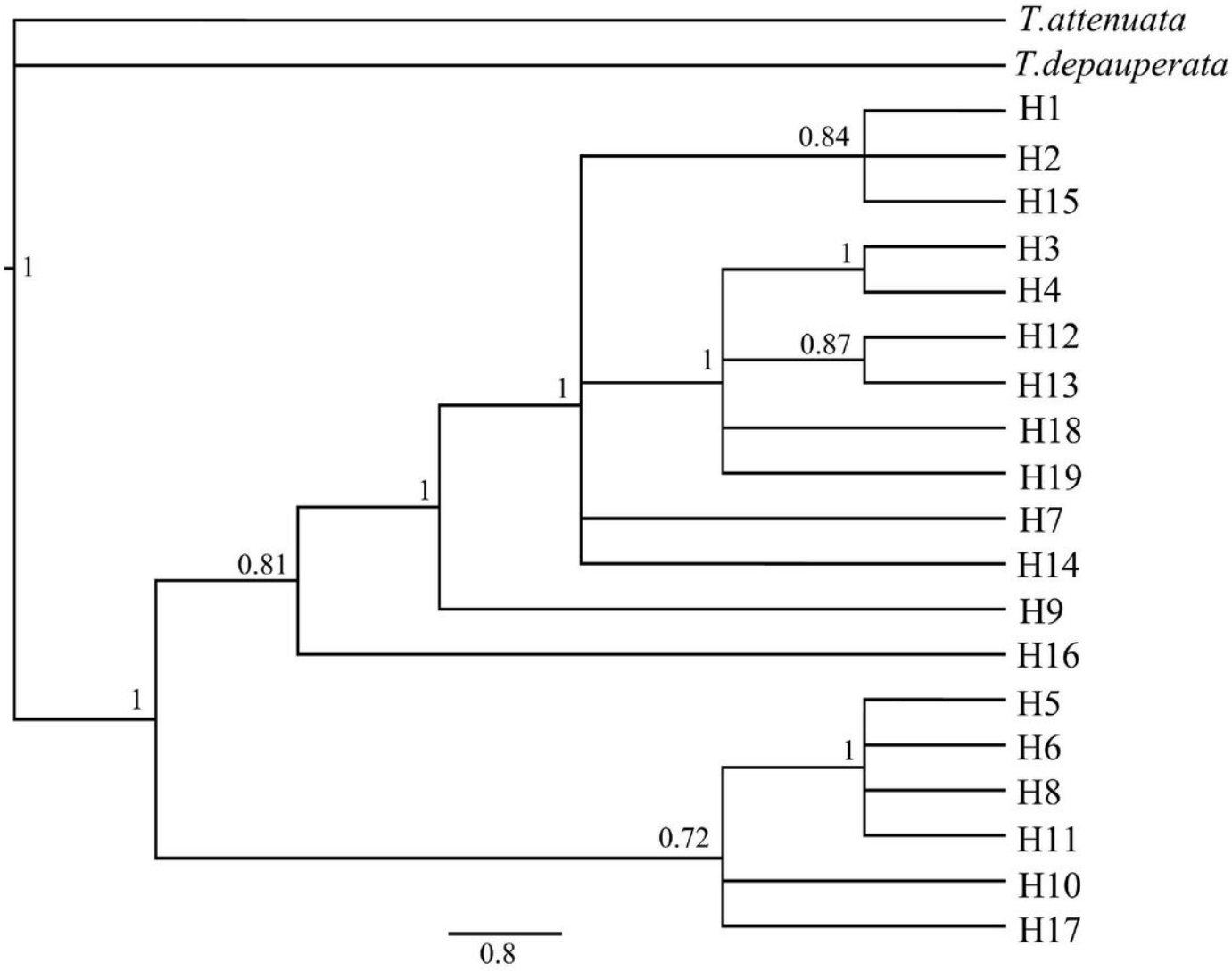

Figure 3

Haplotype bayesian tree of H. lichiangensis based on cpDNA dataset. Tarenna attenuata, Tarenna depauperata were used as outgroups. Numbers above branches indicate posterior probability (PP).

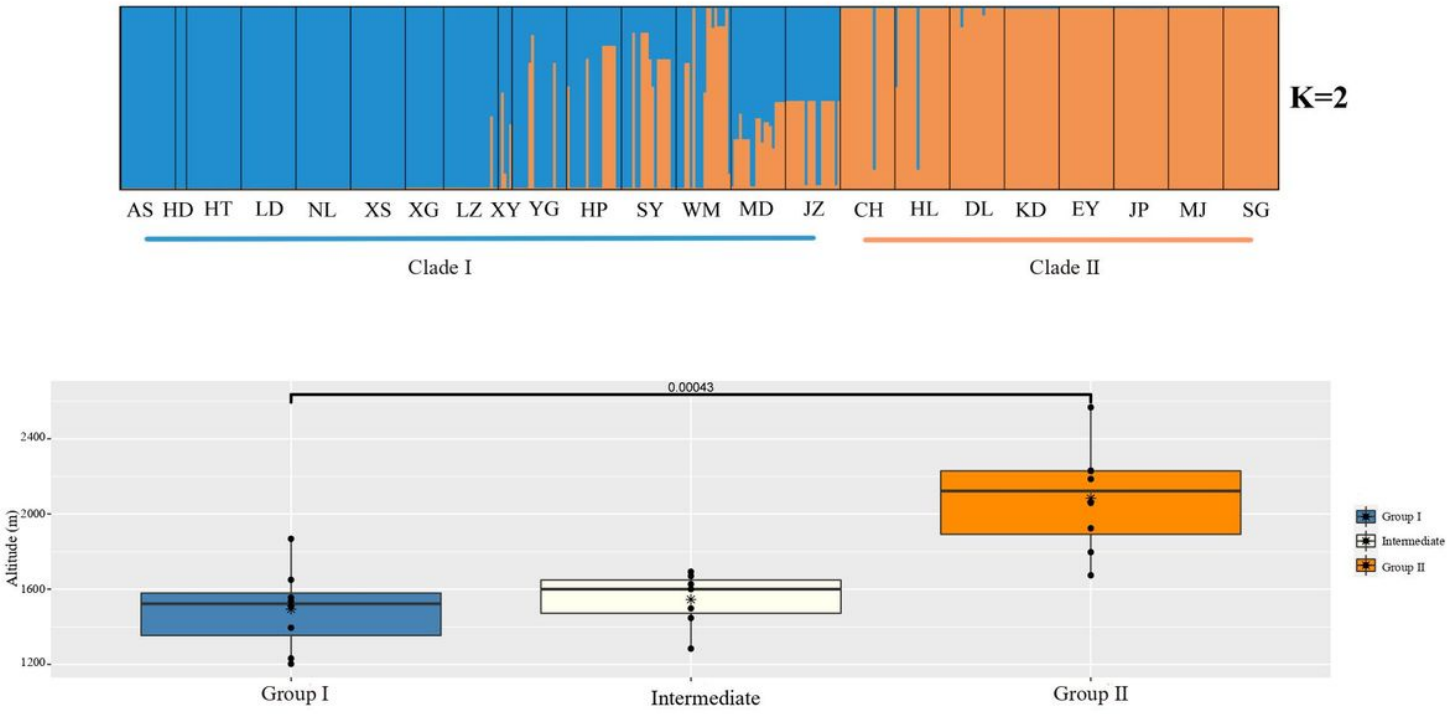

Figure 4

STRUCTURE plot based on bayesian inference with the optimal number of clusters (K = 2) of H. lichiangensis and the resoult of T test.

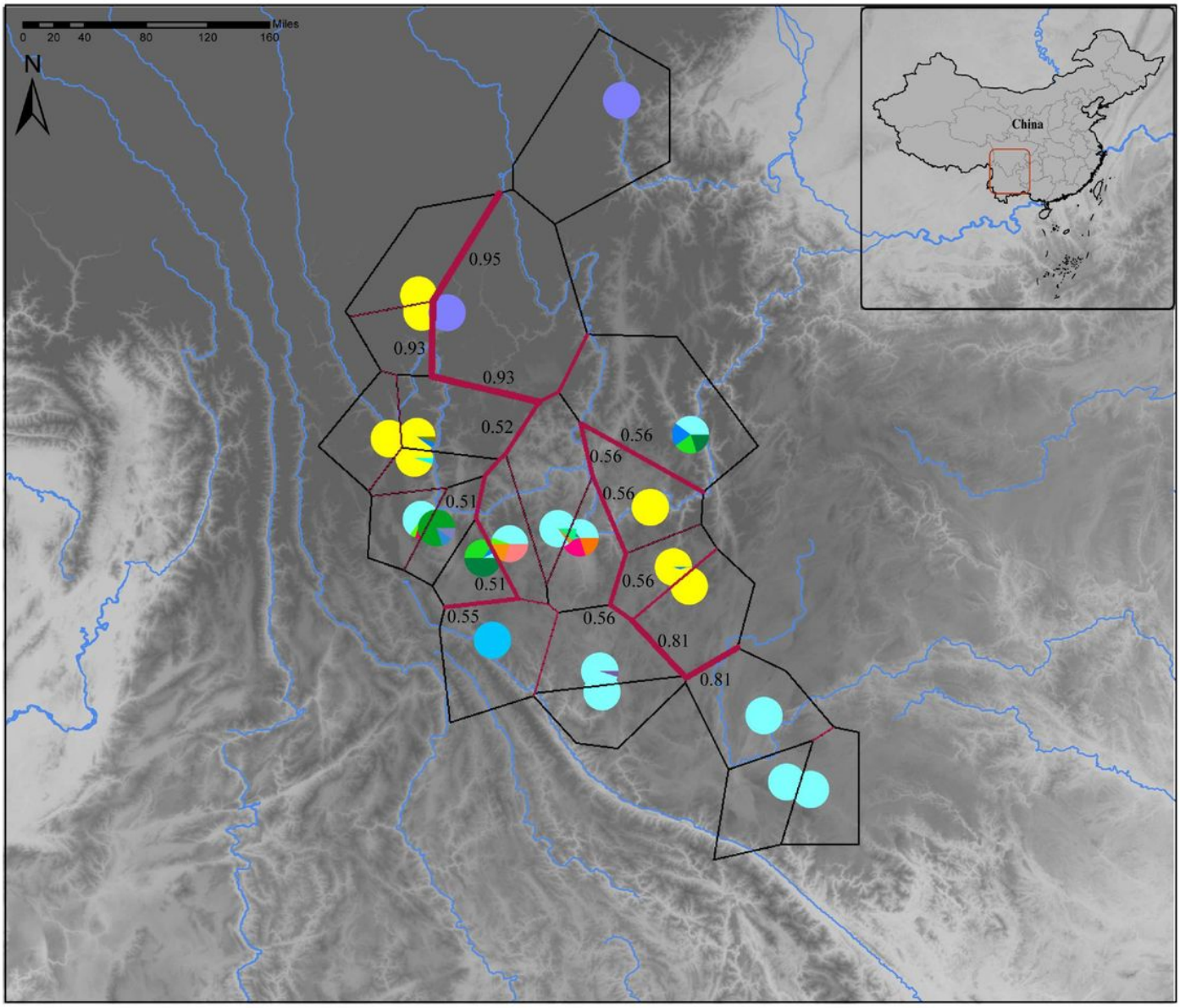

Figure 5

The results of BARRIER analysis. The barriers (heavy red line) detected after performing Barrier on 1000 bootstrapped Nei's genetic distance matrices based on combined nDNA data in H. lichiangensis. Numbers indicate bootstrap support.

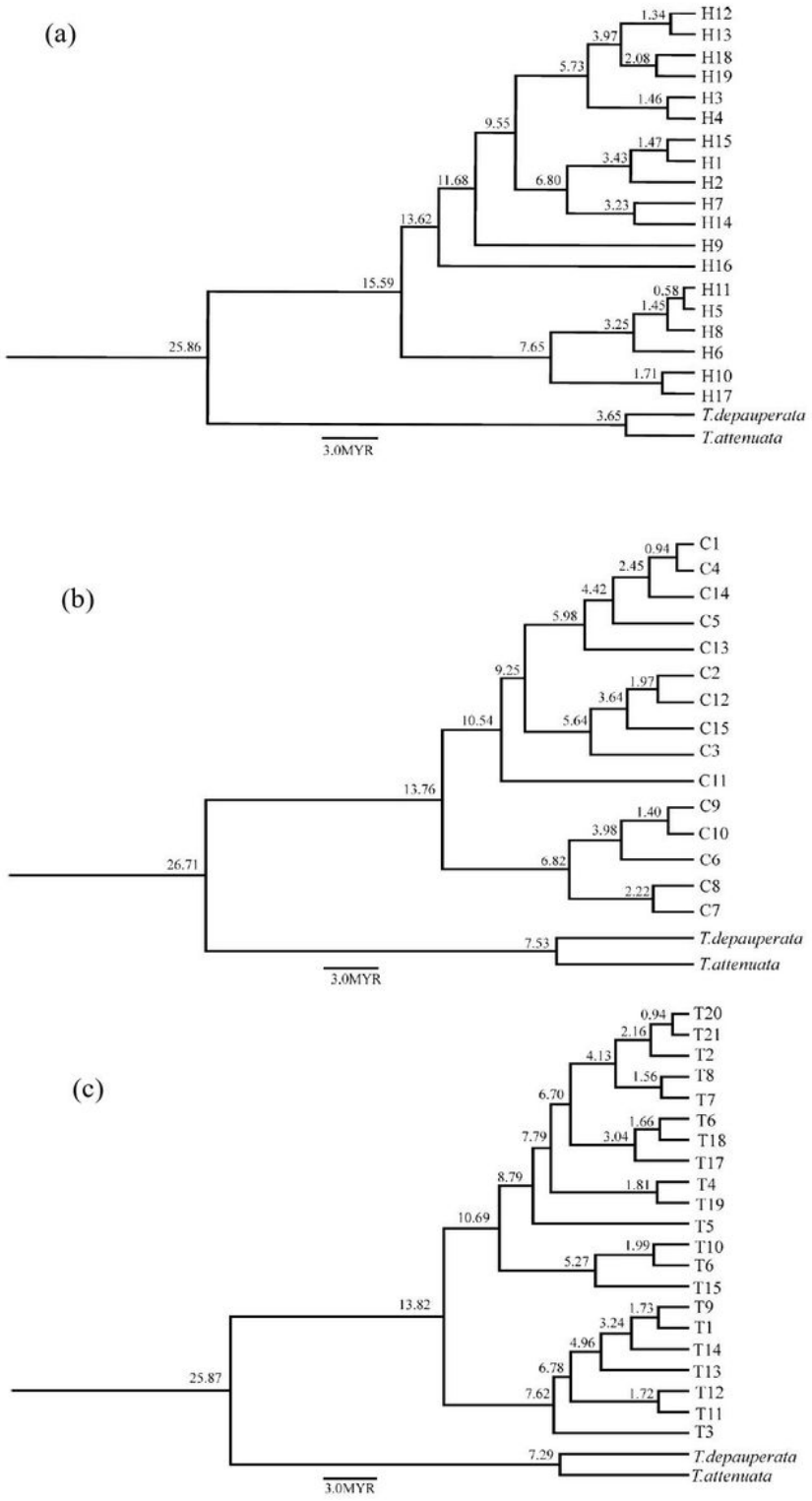

Figure 6

The BEAST-derived trees based on cpDNA and nDNA. The numbers on branches represent divergence time (MYA). (a) cpDNA, (b) CAMX, (c) ITS.

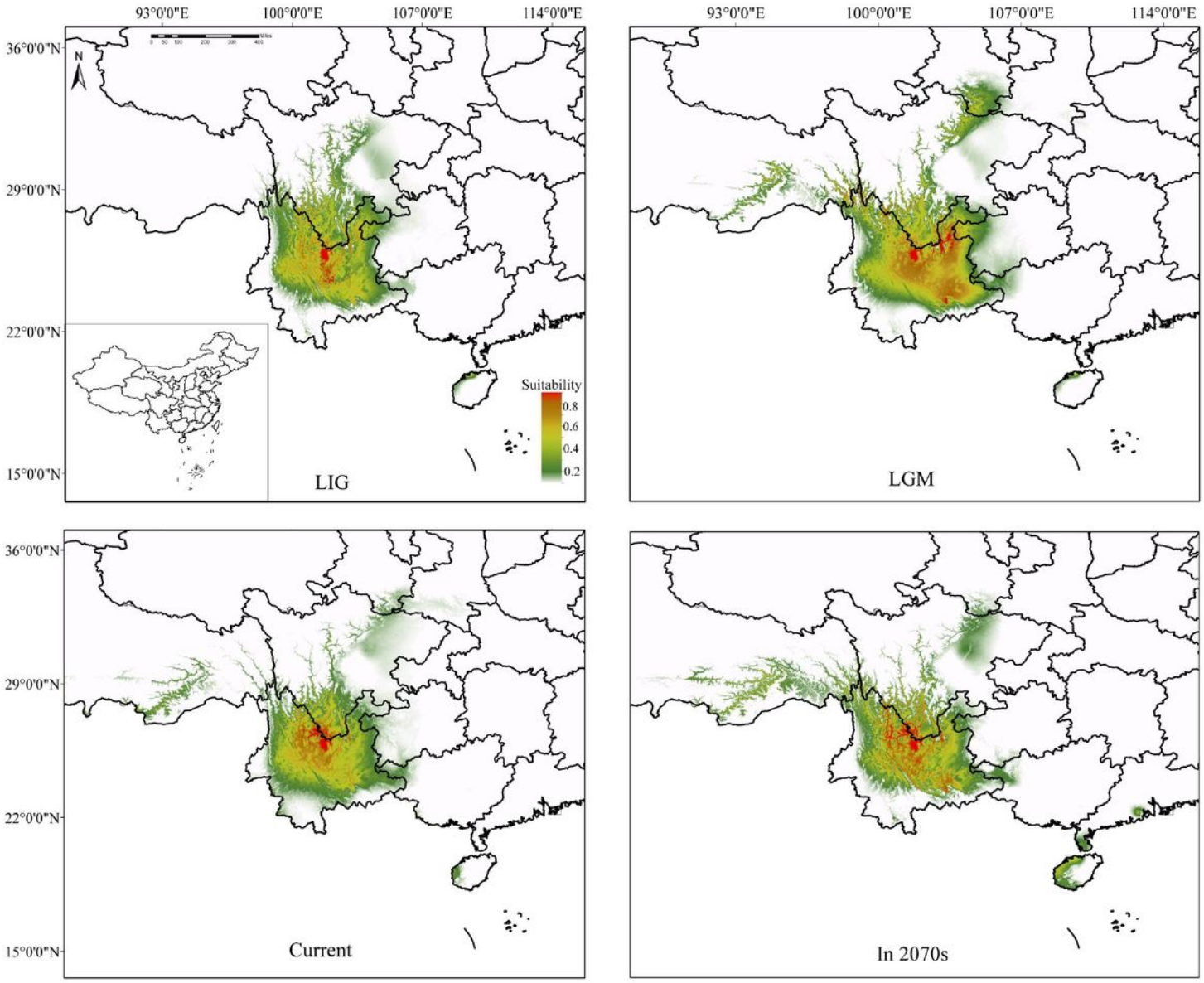

Figure 7

Historical changes of potential distribution areas of H. lichiangensis in four periods based on ecological niche modelling.

Supplementary Files

This is a list of supplementary files associated with this preprint. Click to download.

- FigureS1.pdf
- FigureS2.pdf
- FigureS3.pdf

- TableS1.docx
- TableS2.docx